

Core-corona effect in hadron collisions and muon production in air showers

Sebastian Baur,^{1,*} Hans Dembinski,² Matias Perlin,^{3,4,5} Tanguy Pierog,³ Ralf Ulrich,³ and Klaus Werner⁶

¹*Université Libre de Bruxelles, IIHE – CP230, B-1050 Brussels, Belgium*

²*Max Planck Institute for Nuclear Physics, Heidelberg, Germany*

³*Institute for Nuclear Physics, Karlsruhe Institute of Technology, Karlsruhe, Germany*

⁴*Instituto de Tecnologías en Detección y Astropartículas (CNEA, CONICET, UNSAM), Buenos Aires, Argentina*

⁵*Departamento de Física, FCEN, Universidad de Buenos Aires, Buenos Aires, Argentina*

⁶*SUBATECH, University of Nantes – IN2P3/CNRS – IMT Atlantique, Nantes, France*

(Dated: March 16, 2020)

It is very well known that the fraction of energy in a hadron collision going into electromagnetic particles (electrons and photons, including those from decays) has a large impact on the number of muons produced in air shower cascades. Recent measurements at the LHC confirm features that can be linked to a mixture of different underlying particle production mechanisms such as a collective statistical hadronization (core) in addition to the expected string fragmentation (corona). Since the two mechanisms have a different electromagnetic energy fraction, we present a possible connection between statistical hadronization in hadron collisions and muon production in air showers. Using a novel approach, we demonstrate that the core-corona effect as observed at the LHC could be part of the solution for the lack of muon production in simulations of high energy cosmic rays. To probe this hypothesis, we study hadronization in high energy hadron collisions using calorimetric information over a large range of pseudorapidity in combination with the multiplicity of central tracks. As an experimental observable, we propose the production of energy in electromagnetic particles versus hadrons, as a function of pseudorapidity and central charged particle multiplicity.

Keywords: LHC, collectivity, core-corona, high energy hadron collisions, EPOS, cosmic ray, extensive air shower, muon production

I. INTRODUCTION

Cosmic ray particles reach Earth from galactic and extragalactic sources with enormous energies and produce huge particle cascades in the atmosphere. The resulting extensive air showers are measured with the aim to unveil the astrophysical nature and origin of high energy cosmic rays. The Pierre Auger Observatory [1, 2] and the Telescope Array [3] are the largest contemporary experiments targeting the most energetic cosmic rays with energies beyond 10^{18} eV.

Of particular interest is the cosmic ray mass composition, which is expected to carry a unique imprint of the physics at the sources. The mass composition as a function of the cosmic ray energy E_0 is inferred from air shower observables, of which the most important ones are the depth of the shower maximum X_{\max} and the number of muons N_μ [4]. The depth X_{\max} is the integrated matter density column that a shower traversed until the maximum number of charged particles in the shower is reached. The number of muons is obtained by counting muons when the shower arrives at ground. Experimentally the muon counting is limited to a radial range around the shower axis as well as to a minimal energy of muons.

To infer the cosmic ray mass composition from these observables, accurate predictions from air shower simulations are needed for cosmic rays with various primary

masses. However, the Pierre Auger Observatory [5, 6] and the Telescope Array [7] observed that the measured number of muons in air showers drastically exceeds expectations from model predictions at shower energies around and above 10^{19} eV. A recent summary of muon measurements [8] shows that a consistent muon excess is seen by the majority of cosmic ray experiments over a very wide energy range. The discrepancy between results based on X_{\max} and N_μ is currently preventing an unambiguous interpretation of air shower data in terms of mass composition.

The amount of energy ending up in electromagnetic particles in hadron collisions

$$R = \frac{E_{\text{em}}}{E_{\text{had}}}, \quad (1)$$

where E_{em} is the summed energy over all γ (mostly from π^0 decay) as well as e^\pm , and E_{had} the summed energy of all hadrons, is one of the crucial parameters driving muon production in extensive air showers [9–11]. It is closely related to the way an excited partonic system hadronizes. In hadronic interaction models used to simulate air showers, the hadronization is mainly done using a string fragmentation model which was successfully developed to describe the hadron production in e^+e^- collisions, and low energy proton-proton collisions. In systems with higher energy densities, such as heavy ion collisions, a statistical hadronization of a fluid is expected where the production of heavy particles is favored, thus, reducing the fraction of π^0 compared to other types of particles. In the early 2000s “collective effects” have been observed in heavy ion collisions (often referred to as *large* systems) at

* sebastian.baur@ulb.ac.be

RHIC [12–15]. Similar effects have been predicted [16–21] for proton-proton collisions (aka *small* systems) and were eventually discovered at the LHC [22] (see Refs. [23, 24] for detailed reviews).

While a fluid-like behavior (referred to as collective effects in the following) is confirmed in both large and small systems, their origin is still unclear. In large systems the existence of a quark-gluon-plasma (QGP) is commonly assumed as a phase of parton matter where confinement is no longer required [25–27]. This QGP will evolve according to the laws of hydrodynamics and eventually decay statistically. There are various expected consequences of such a scenario, such as long-range two-particle correlations, the so-called “ridge” phenomenon [22, 28], jet quenching [29, 30], or enhanced production of strange hadrons [31]. It was initially a surprise when such effects were also discovered in small systems. While it was argued that also in central collisions of small systems the energy densities may be high enough to allow for the formation of a QGP [16], other recent studies have shown that collective effects can be achieved by alternative mechanisms such as microscopic effects in string fragmentation [32] or QCD interference [33]. The possibility of collective effects in smaller systems opens the door to study the impact of a different hadronization scheme in high energy interactions also within air showers. Air shower cascades are driven by collisions of hadrons and light nuclei at ultra-high energies. We show that statistical hadronization in collisions of hadrons and nuclei can play a so far underestimated importance in the understanding of muon production in air showers [34, 35].

The underlying mechanism responsible for the production of these effects is expected to produce characteristic observables in the final state of hadron collisions. We demonstrate how statistical hadronization affects the energy fraction contained in electromagnetic versus hadronic particles, R , and show how this has important possible implications for the muon production in cosmic ray air showers.

We further propose detailed measurements of R as a novel opportunity to study collective hadronization in small systems at the LHC. This may lead to a better understanding of the underlying nature of statistical hadronization since different theoretical approaches lead to predictions that may be distinguished based on measurements. In addition those measurements are able to constrain models for air shower simulations.

II. THE MUON PROBLEM AND THE R OBSERVABLE

The dominant mechanism for the production of muons in air showers is via the decay of light charged mesons. The vast majority of mesons are produced at the end of the hadron cascade after typically five to ten generations of hadronic interactions (depending on the energy and zenith angle of the cosmic ray). The energy carried

by neutral pions, however, is directly fed to the electromagnetic shower component and is not available for further production of more mesons and subsequently muons. The energy carried by hadrons that are not neutral pions is, on the other hand, able to produce more hadrons and ultimately muons in following interactions and decays. Using a simple Heitler type toy-model [36] based on [37], the *neutral pion fraction* $c = N_{\pi^0}/N_{\text{mult}}$, defined as the number of neutral pions N_{π^0} divided by the total number of final-state particles N_{mult} in a collision, was found to have a strong impact on the muon number and in particular on the slope of the energy dependence of the muon production. Indeed in this model we get

$$N_{\mu} = \left(\frac{E_0}{E_{\text{dec}}} \right)^{\beta} \quad \text{with} \quad \beta = 1 + \frac{\ln(1-c)}{\ln N_{\text{mult}}}, \quad (2)$$

where E_0 is the energy of the primary cosmic ray particle and E_{dec} is the typical energy at which mesons decay in the cascade. So the muon number N_{μ} increases strongly with decreasing c , which is understandable since more hadrons is available to produce muons. A second quantity with a strong impact on the muon number was identified to be the hadron multiplicity N_{mult} .

The value of c is very important for the muon production. Unfortunately, it is difficult to measure both N_{π^0} and N_{mult} experimentally (for example at the LHC) since neutral particles cannot be easily counted individually. In general, secondary particle identification is unavailable at large pseudorapidities η where the energy flow is large enough to become relevant for the air shower development. Hence, we propose a new observable which is sensitive to properties of the hadronization and which can be directly related to c : the ratio of the electromagnetic to the hadronic energy density R given by

$$R(\eta) = \frac{\langle dE_{\text{em}}/d\eta \rangle}{\langle dE_{\text{had}}/d\eta \rangle}. \quad (3)$$

Here the energy densities $\langle dE/d\eta \rangle$ are obtained by summing the energy of all final-state particles except for neutrinos in bins of η and averaging over a large number of collisions.

The neutral pion fraction c can be easily related to the energy ratio R , since both are very similar kinematic aspects of final state distributions. If all particles have the same energy such as in the generalized Heitler model, then we have simply $R = c/(1-c)$. But R is experimentally much easier to measure, since, using a calorimeter, the signals deposited by electromagnetic particles and by hadrons are characteristically different. We compute a detailed conversion between R and c using standalone EPOS LHC [38] simulations of fixed energy proton-proton collisions at various center-of-mass energies, and found that for the relevant parameter range, a change of R by ΔR affects c by $\Delta c \approx 0.8 \cdot \Delta R$, where R is computed by integrating eq. (3) over all η . In section IV, we will study R for different models as a function of η , and at fixed η as a function of the charged particle density at central

pseudorapidity $dN_{\text{ch}}/d\eta|_{\eta=0}$, which is determined as the average multiplicity within $|\eta| < 0.5$.

The influence of various effective parameters q in interaction models (like R , c , or N_{mult}) on the main air shower observables was investigated in a previous study [9] in which the behavior of hadronic interaction models in air shower simulations was modified in an energy-dependent way during full air shower cascade simulations within CONEX [39].

The effective quantity q of the hadronic event generators inside the air shower cascade simulation is changed in an energy dependent way

$$q(E_{\text{lab}}) \rightarrow q(E_{\text{lab}}) \times (1 + f_q F(E_{\text{lab}}; E_{\text{th}}, E_{\text{scale}})) \quad (4)$$

using the modification scale f_q , and the energy-dependent factor

$$F(E_{\text{lab}}; E_{\text{th}}, E_{\text{scale}}) = \frac{\log_{10}(E_{\text{lab}}/E_{\text{th}})}{\log_{10}(E_{\text{scale}}/E_{\text{th}})} \text{ for } E_{\text{lab}} > E_{\text{th}}, \quad (5)$$

representing the assumption that models are well constrained by accelerator data at lower energies (below E_{th}), where $F(E_{\text{lab}}) = 0$, while they become logarithmically unconstrained going to higher energies. The parameter E_{scale} is the *reference* energy scale. We will use $E_{\text{scale}} = E_{\text{LHC}}^{\text{CR}} \simeq s_{\text{LHC}}/(2m_p) \approx 90 \text{ PeV}$, using an LHC center-of-mass energy of 13 TeV. Typical threshold values are $E_{\text{th}} \simeq s_{\text{Tevatron}}/(2m_p) \approx 1 \text{ PeV}$, using the center-of-mass energy of the Tevatron accelerator. However, in particular particle production, in the important forward phase space, may be largely unconstrained by both Tevatron and LHC data, allowing much lower values of E_{th} to be explored. It is a key point of the application of eq. (5) inside CONEX that a significant fraction of the air shower cascade is consistently modified during the simulations.

We apply eqs. (4,5) to explore the correlated impact of $q = R$ and $q = N_{\text{mult}}$ on X_{max} and $\ln N_{\mu}$ in full air shower simulations. The resulting correlated effect is shown in Fig. 1 as demonstrated for air showers at $E_0 = 10^{19} \text{ eV}$ using EPOS LHC in CONEX. Lines in this figure show all possible resulting mean values of X_{max} and $\ln N_{\mu}$ for any mass composition of cosmic rays between pure proton (bottom right end of lines) and pure iron (top left end of lines). The resulting values of X_{max} and $\ln N_{\mu}$ are located on a straight line because the mean values for both are linear functions of the mean-logarithmic mass of cosmic rays [40, 41] given a fixed air shower energy. The line-shape is universal, but its location, and to a lesser degree the slope and length, depend on the hadronic interaction model. Current hadronic interaction models predict lines, which are too low compared to experimental data from air showers, as indicated by the vertical gap between the representative data point from the Pierre Auger Observatory [5] and the EPOS LHC line. This discrepancy is the expression of the muon problem outlined above.

When N_{mult} is modified the simulated line shifts along itself: the multiplicity has a correlated effect on X_{max}

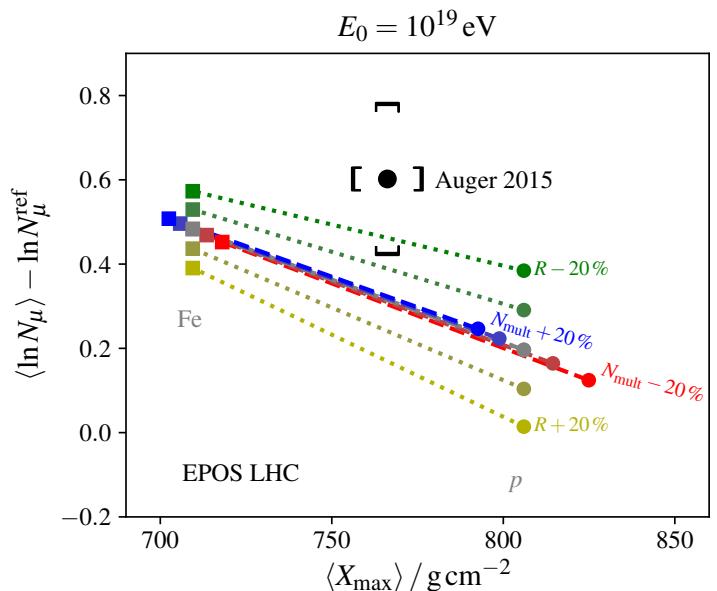


FIG. 1. Impact of the modification scales f_q (in %) of the hadron multiplicity N_{mult} (dashed lines) and the energy ratio R (dotted lines) in collisions at the LHC energy of $\sqrt{s} = 13 \text{ TeV}$ on EPOS LHC predictions of the air shower observables X_{max} and $\ln N_{\mu}$ in 10^{19} eV air showers. The datum is from the Pierre Auger Observatory [5]. The model lines represent all values that can be obtained for any mixture of cosmic nuclei from proton (bottom right) to iron (top left).

and $\ln N_{\mu}$ that cannot close the gap to the data. However, modifications of R mainly affect the muon number and leave X_{max} unchanged, creating vertical shifts and tilts of the line in the plot. Thus, within the assumptions outlined here, we find that a decrease of R by $f_q = -15\%$ at the LHC energy of $\sqrt{s} = 13 \text{ TeV}$ would be sufficient to make the simulations compatible with the air shower data at 10^{19} eV . These results have been cross-checked with alternate interaction models in the air shower simulations. There is a very good qualitative agreement in all cases.

Furthermore, in Ref. [8] it was established that the muon discrepancy in simulations increases smoothly with energy. Thus, the slope of the energy dependence introduced in eq. (2) is also affected, pointing to a too small value of β . This may be related to a too large π^0 production. We explore this energy dependence in more detail in the next section.

III. CORE-CORONA EFFECT AND MUON PROBLEM

The discussion in the previous section suggests that a change of R (or c , which is equivalent) is a potential way to reduce the discrepancy between measurements and air shower simulations. Nevertheless, R is quite well constrained by theory as well as laboratory measurements

and, thus, can not be changed entirely arbitrarily as studied in the previous section II. In a naive model like Ref. [37] where only pions are considered as secondary particles, $R = 0.5$. In a more realistic approach based on string fragmentation we have $R \approx 0.41$. But as shown in Ref. [31], particle ratios such as K/π , p/π or Λ/π change with increasing secondary particle density, saturating to the value given by a thermal/statistical model with a freezeout temperature of 156.5 MeV [42] yielding $R \approx 0.34$. Such a behavior can be explained in terms of a core-corona picture [43]. This approach has been used in the framework of realistic simulations [44], but also in simple model calculations [45–48]. The basic idea is that some fraction of the volume of an event (or even a fraction of events) behaves as a quark gluon plasma and decays according to statistical hadronization (core), whereas the other part produces particles via string fragmentation (corona). The particle yield N_i for particle species i is then a sum of two contributions

$$N_i = \omega_{\text{core}} N_i^{\text{core}} + (1 - \omega_{\text{core}}) N_i^{\text{corona}}, \quad (6)$$

where N_i^{core} represents statistical (grand canonical) particle production, and N_i^{corona} is the yield from string decay. Crucial is the core weight ω_{core} . In order to explain LHC data [31] the weight ω_{core} needs to increase monotonically with the multiplicity, starting from zero for low multiplicity pp scattering, up to 0.5 or more for very high multiplicity pp, reaching unity for central heavy ion collisions (PbPb).

In the following, we are going to employ a straightforward core-corona approach, based on eq. (6), for any hadronic interaction model in CONEX air shower simulations. The particle yield from the chosen interaction model is by definition considered to be the corona yield, whereas we use the standard statistical hadronization (also referred to as resonance gas) for the core part. So $\omega_{\text{core}} = 0$ would be the “normal” simulation with the default interaction model. Choosing $\omega_{\text{core}} > 0$ amounts to mixing the yields from the interaction model according to the core-corona superposition shown in eq. (6). The core will certainly help concerning the “muon problem”, because statistical hadronization produces more heavy particles and less pions compared to string fragmentation, and therefore R is smaller [34, 35].

Technically, we directly modify individual particle ratios of the secondary particle spectra dN_i/dE_j , for particle species i and energy bins dE_j , of hadronic interactions with air nuclei used by CONEX for numerical air shower simulations based on cascade equations. Knowing the initial ratios π^0/π^\pm , p/π^\pm , K^\pm/π^\pm , p/n , K^0/K^\pm (taking into account strange baryon decays) from a corona type model and the value of the same ratios from the core model, we compute new spectra in which the particle yields include both, core and corona according to ω_{core} . Since the hadronization mechanism can affect only newly produced particles the properties of the leading particle should be preserved. To achieve that, the new particle yields are computed for all secondaries, but excluding

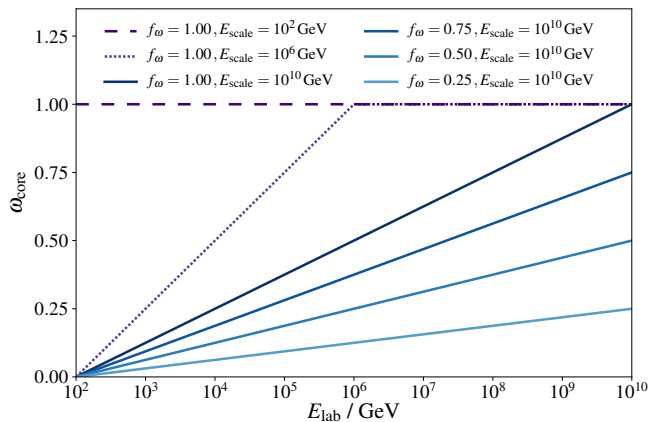


FIG. 2. Different energy evolutions probed for ω_{core} . The solid lines represent changing the scale f_ω of the effect, while the dashed lines also indicate the effect of changing E_{scale} .

the one corresponding to the respective projectile type, i.e. protons in proton-air, kaons in kaon-air interactions, and so on. The yield of the projectile-type particles is determined subsequently by exploiting energy conservation in all energy bins dE_j summed over all secondary particle species i : the sum $\sum_i E_j dN_i/dE_j$ must be conserved. Since at high $x_F = E_j/E_{\text{lab}}$ only the projectile-type particles will have dN_i/dE_j significantly different from zero (aka leading-particle effect), the resulting modified leading-particle type spectra at high x_F follow the original distribution, and are only affected by the scaling procedure at lower values of x_F . Together, this assures that energy conservation as well as the total multiplicity are not affected, but only the particle ratios. More details will be given in a future publication.

We expect the core weight ω_{core} to increase with energy in a logarithmic way. Thus, we use

$$\omega_{\text{core}}(E_{\text{lab}}) = f_\omega F(E_{\text{lab}}; E_{\text{th}}, E_{\text{scale}}) \quad (7)$$

to model this (in analogy to eq. (4)), starting already at fixed-target energies, $E_{\text{th}} = 100$ GeV. Different energy dependencies are explored by changing E_{scale} from 100 GeV (corresponding to a step function), to 10^6 GeV, and 10^{10} GeV. The f_ω scale is varied from 0.25, 0.5, 0.75 to 1.0; in addition we enforce $F(E_{\text{lab}}; E_{\text{th}}, E_{\text{scale}}) \stackrel{!}{=} 1$ for all $E_{\text{lab}} \geq E_{\text{scale}}$. This yields the ω_{core} energy dependencies as depicted in Fig. 2. All these scenarios have been used to simulate full air showers with CONEX, using cascade equations from the first interaction to the ground, for proton and iron primary particles at $E_0 = 10^{19}$ eV. In Fig. 3 the results are shown in the $X_{\text{max}} - \ln N_\mu$ plane for two models EPOS LHC (left) and QGSJETII.04 [49, 50] (right). These examples illustrate that it is well possible with modified hadronization in air shower cascades to describe the data of the Pierre Auger Observatory. As expected, more core-like contributions are needed compared to what is currently provided by the models. This means, QGP-like effects also in light colliding systems

and starting in central collisions at much lower center-of-mass energies may play a decisive role.

Furthermore, from eq. (2) also a different energy evolution of the muon production follows. To study the effect of our core-corona model on the muon production as a function of the energy, we can compare the different scenarios with the compilation of data presented in Ref. [8] using the renormalized factor

$$z = \frac{\langle \ln N_\mu \rangle - \langle \ln N_\mu \rangle_{\text{p}}}{\langle \ln N_\mu \rangle_{\text{Fe}} - \langle \ln N_\mu \rangle_{\text{p}}}, \quad (8)$$

with N_μ being any muon related experimental observable and $\langle \ln N_\mu \rangle_{\text{p}}$ and $\langle \ln N_\mu \rangle_{\text{Fe}}$ being the average of the logarithm of the same observable simulated with proton and iron primaries respectively for a given reference hadronic interaction model. This allows a direct comparison between different experiments for various types of muon observables.

Considering the energy dependence of z , there is an implicit dependence on the cosmic-ray mass A , since $\langle \ln A \rangle$ varies with energy. However, as expected from the Heitler model formula, and even more importantly, verified via explicit simulations, z and $\langle \ln A \rangle$ are related as $z = a + b\langle \ln A \rangle$, and from $z(\text{pure Fe}) = 1$ and $z(\text{pure p}) = 0$ we simply get $a = 0$ and $b = 1/\ln 56$. This is very useful, since it means that the A -dependence of z (called z_{mass}) is given as

$$z_{\text{mass}} = \frac{\langle \ln A \rangle}{\ln 56}, \quad (9)$$

and the expectation of $\Delta z = z - z_{\text{mass}}$ is zero for the case of full consistency between all experimental observables and the simulations based on a valid reference model. This means, plotting Δz for experimental data, we should get zero if the reference model were perfect, whereas $\Delta z > 0$ implies a muon deficit in the simulations. In this way we can visualize the energy dependence of the muon excess, corrected for mass dependencies. More details and references are given in Ref. [8].

As pointed out in Ref. [8], for all models the data have a positive Δz showing a significant logarithmic increase with the primary energy, indicating an increasing muon deficit in the simulations. In Fig. 4 the effect of the different energy evolution of ω_{core} for EPOS LHC and QGSJETII.04 on Δz are shown. Here the new simulations are treated like data and the z factor is calculated using the original (quoted) models as a reference such that the new Δz can be compared to the data points directly. The positive Δz of the lines indicate a larger muon production when ω_{core} increases and the positive slopes mean that the slope of the muon production as a function of the primary energy is larger when ω_{core} increases. By including a consistent core-like hadronization, we thus reproduce the energy evolution as found in the data. This is even possible for values $\omega_{\text{core}} < 1$.

The possibility to see the effect of a core hadronization (QGP or similar more exotic phenomena) on air shower

physics have already been studied in the literature [51–54]. Changes in the muon production because of a change of R under either extreme or exotic assumptions (which were not yet observed at the LHC) are usually assumed. Furthermore, it was shown that the production of a core only in very central, high-density, collisions is not sufficient to significantly change the muon numbers in air shower simulations [55].

In contrast to the new results presented here, in those previous studies the core-like production does not cover sufficient phase space to change the muon production in air showers significantly. We demonstrate that core-like effects potentially starting at much smaller colliding systems, and at much lower center-of-mass energies as studied here, have an important impact on muon production in air showers. There are various indications at the LHC in pp and pA collisions that such a scenario is compatible with current data [22, 31], or even suggested by it, at energy densities as reached by cosmic rays interacting with the atmosphere [35]. Studying LHC data at mid-rapidity it is found that for events with $\langle dN_{\text{ch}}/d\eta \rangle_{|\eta| < 0.5} \sim 10$ (corresponding to typical proton-air interactions) ω_{core} is already $\approx 50\text{--}75\%$. Since our study is based on the simple assumption that the full phase space has a modified π^0 ratio, it remains crucial for cosmic ray physics to conduct further dedicated measurements at the LHC to better understand π^0 production relative to other particles. The phase space for the formation of core-like effects is potentially significantly larger than previously studied, and in particular may extend towards larger rapidities.

IV. TESTING CORE CONTRIBUTIONS VIA MEASUREMENTS OF R AT THE LHC

As previously outlined an enhanced contribution of core-like hadronization can help to explain the data of the Pierre Auger Observatory. In the following we discuss how this can be probed with accelerator data.

We mainly use EPOS LHC as the baseline model to test sensitivity towards a QGP-like state. As alternative model we use PYTHIA8 [56, 57], which provides entirely different (non-QGP-like) physics concepts for collectivity. EPOS LHC is a general purpose event generator widely used in high energy physics, and in particular also for heavy ion collisions. It includes the description of a QGP-like behavior in high energy collisions. PYTHIA8, on the other hand, is the reference model in high energy physics for proton-proton interactions. Both models generate a distribution of colored strings from the collision of a projectile and a target. Despite a very different underlying approach for the string generation (pQCD factorization for PYTHIA8 and parton-based Gribov-Regge theory [58] for EPOS LHC), the string distributions are not very different, because they are strongly constrained by the data on particle multiplicities. These strings can be hadronized directly in both generators using the Lund string model [59] in PYTHIA8, or the area

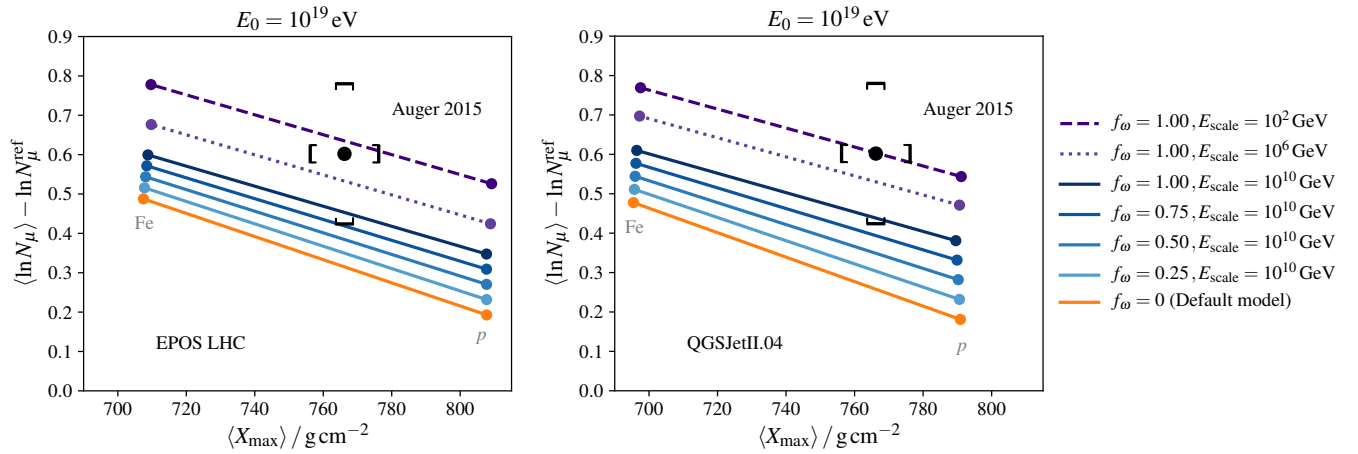


FIG. 3. Comparison of different core-corona mixing scenarios, as described in the text, on air shower simulations at 10^{19} eV using EPOS LHC (left) and QGSJETII.04 (right) in the $X_{\text{max}} - \ln N_\mu$ plane. The solid lines represent changing the scale f_ω , while the dashed lines also indicate the effect of changing E_{scale} . The *default* model corresponds to the corona-only simulations. The datum is from the Pierre Auger Observatory [5]. Each model line represents all values that can be obtained for any mixture of cosmic nuclei from proton (bottom right) to iron (top left).

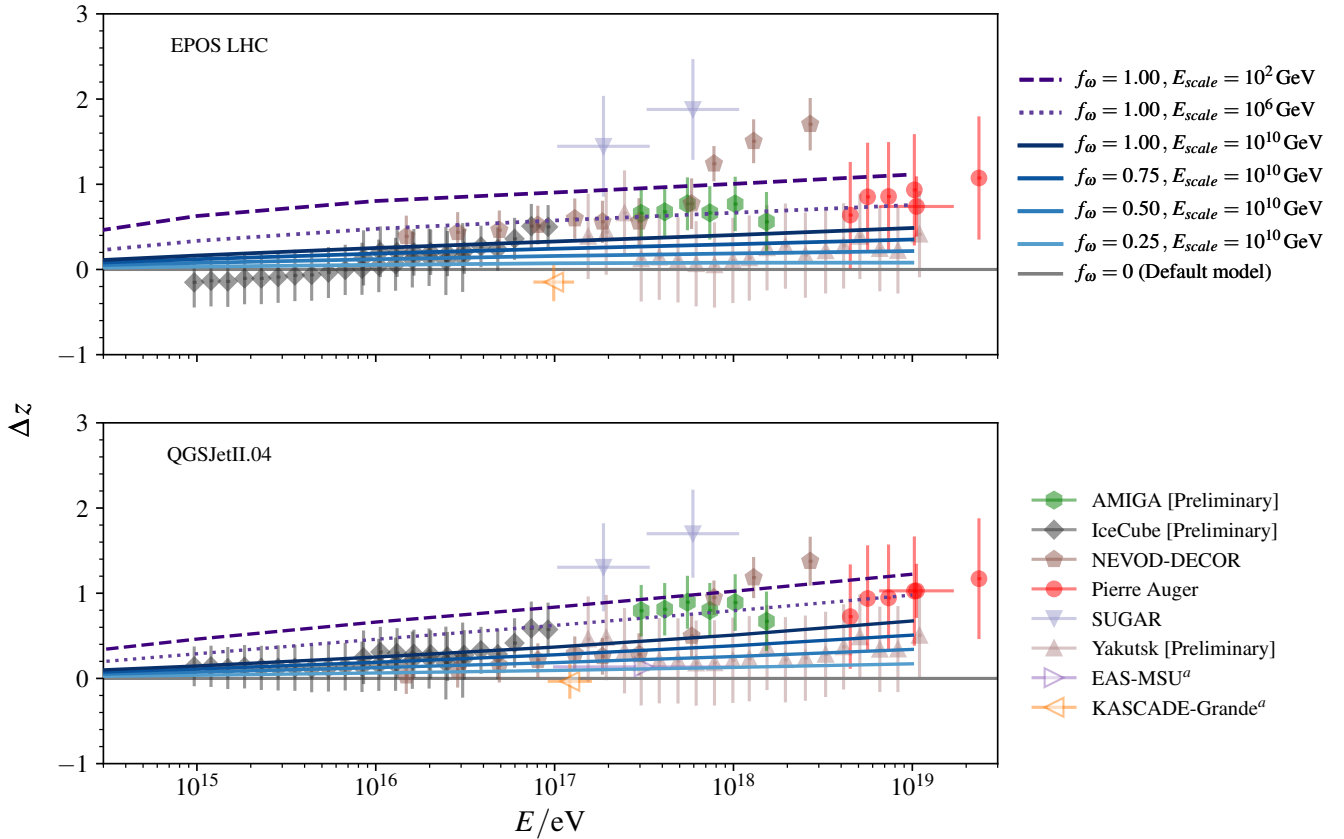


FIG. 4. Evolution of the mass corrected z -factor, $\Delta z = z - z_{\text{mass}}$, as a function of the primary energy. The data are taken from Ref. [8] and references therein. Overlaid are predictions obtained from changing the scale f_ω (solid lines) and E_{scale} (dashed and dotted lines) obtained with EPOS LHC (top) and QGSJETII.04 (bottom) air shower simulations.

law [58] in EPOS LHC – both cases are strongly constrained by LEP data. At low energy (≈ 10 to 100 GeV) this is sufficient to successfully describe proton-proton interactions with good accuracy. Nevertheless, it turns out that at the LHC additional physics mechanisms are needed to describe the observed particle correlations and abundances in the final state. In PYTHIA8, a modified color reconnection approach [60, 61] or a “string shoving” mechanism [32] have been proposed to introduce collective effects such as a modified hadronization or particle correlations, similar to those obtained from a QGP. In EPOS LHC, on the other hand, the “core-corona” approach [44] is used as originally developed for heavy ion collisions. As already explained, the core amounts to areas with high string/energy densities, where strings are assumed to “melt” and produce matter that expands hydrodynamically and then decays statistically, whereas the corona represents particles from ordinary string fragmentation, which escape from the dense regions. While in EPOS3 [62] the hydrodynamic expansion is fully implemented and hadronization occurs on a freeze-out hypersurface, in EPOS LHC this expansion is mimicked by parameterizing the flow at hadronization. This has proven to describe various collective observables well [38]. Simulations of EPOS LHC are readily available via the CRMC software [63]. On generator level, we study particles with a lifetime $c\tau > 1$ cm, which is consistent with most experimental detector designs.

In fact, in EPOS LHC final-state particles originate from three different production mechanisms: standard string fragmentation (corona), statistical decay of a fluid (core), and the decay of the beam remnants. While experimentally the origin of the production mechanism for a particle cannot be identified, individual production mechanisms can still be studied since they predominantly contribute to different regions of phase space. This is demonstrated in Fig. 5 (top), which shows the relative contribution of these mechanisms to the total energy density $\langle dE/d\eta \rangle$ for minimum bias proton-proton collisions at a center-of-mass energy of 13 TeV. Three regions can be identified: The energy density at central pseudorapidities, $|\eta| < 5$, is dominated by particles originating in the dense core of the interaction, at intermediate rapidities, $5 < |\eta| < 8$, it is dominated by particles from string fragmentation, and at large rapidities, $|\eta| > 8$, by the fragmentation of beam remnants. Underlying differences in particle production, therefore, lead to varying observables as a function of pseudorapidity.

A corresponding effect is also observed as a function of the central charged particle multiplicity N_{ch} . Final states with large particle multiplicity are known to be an effective trigger for pronounced statistical hadronization [22]. Therefore, at fixed pseudorapidity, the influence of the core increases as a function of particle multiplicity. This effect is expected to be most significant at $|\eta| \approx 0$ since the relative contribution of the core is largest. This is illustrated in the middle panel of Fig. 5 for $\eta = 0$ and in the bottom panel for $\eta = 6$. It can be seen that the contribu-

tion of the core to the energy density at $\eta = 0$ becomes dominant for pp collisions with more than ≈ 7 charged particles per unit of pseudorapidity, while at $\eta = 6$ this transition is shifted to a larger number.

Using EPOS LHC we find that the fraction of secondary pions in the dense core is reduced because many other more massive hadrons and resonances are produced. This leads to a lower ratio of the electromagnetic to hadronic energy density in particles produced from the core. Accordingly, this effect can be seen in the pseudorapidity-dependent ratio of the average electromagnetic to hadronic energy density R shown in top panel of Fig. 6. At $|\eta| \approx 0$, the energy density is dominated by the core and therefore the value of R for EPOS LHC is as low as 0.34 . As the contribution of the core to the total energy decreases with increasing pseudorapidity, also R increases and reaches a value of 0.4 at $|\eta| \approx 7$ before it decreases rapidly due to the very low electromagnetic contribution in the beam remnants. In comparison, a flat ratio below $|\eta| \approx 7$ is obtained when statistical hadronization is disabled in EPOS LHC (corona only). The data point shown in this figure at $\eta \approx 6$ is derived from Ref. [64], where we have corrected the original values from detector level to generator level using the Rivet routines provided by the CMS Collaboration [65]. The shaded region corresponds to the systematic uncertainties of the measurement. These data are consistent with all models within the experimental uncertainty; there is a slight tension with the PYTHIA8 simulations using the modified colour reconnection approach [66]. Such data with smaller uncertainties, and measured over a wide range of η have the potential to differentiate between some of the models. In particular, any slope observed in the region $0 < |\eta| \lesssim 6$ would be a clear hint for a transition of several distinct hadronization mechanisms (i.e. core-corona).

The ratio of the electromagnetic to hadronic energy density R at $\eta = 0$ is shown as a function of the central multiplicity $dN_{\text{ch}}/d\eta|_{\eta=0}$ in the middle panel of Fig. 6. It can be observed that R drops down to values of 0.3 when statistical hadronization is enabled in EPOS LHC while it reaches a constant plateau of 0.4 in the case of disabled statistical hadronization, which is similar to the PYTHIA8 predictions. At $\eta = 6$, it can be seen in the bottom panel of Fig. 6 how the different model predictions compare to the available CMS data (also from Ref. [64]). However, these data are taken at $\eta \sim 6$, were one can see from Fig. 6 (top) that the sensitivity to model differences is unfortunately close to minimal. It would be a great way to study hadronization in hadron collisions by measuring this at LHC in a much wider η region.

We compare the simulations obtained with EPOS LHC also to predictions by PYTHIA8 in the standard minimum bias configuration as well as with modified QCD-based color reconnection parameters as presented in Ref. [61], and enabled string shoving mechanisms. For the latter we use the example parameters provided within PYTHIA8 version 8.235. We are aware that these settings are un-

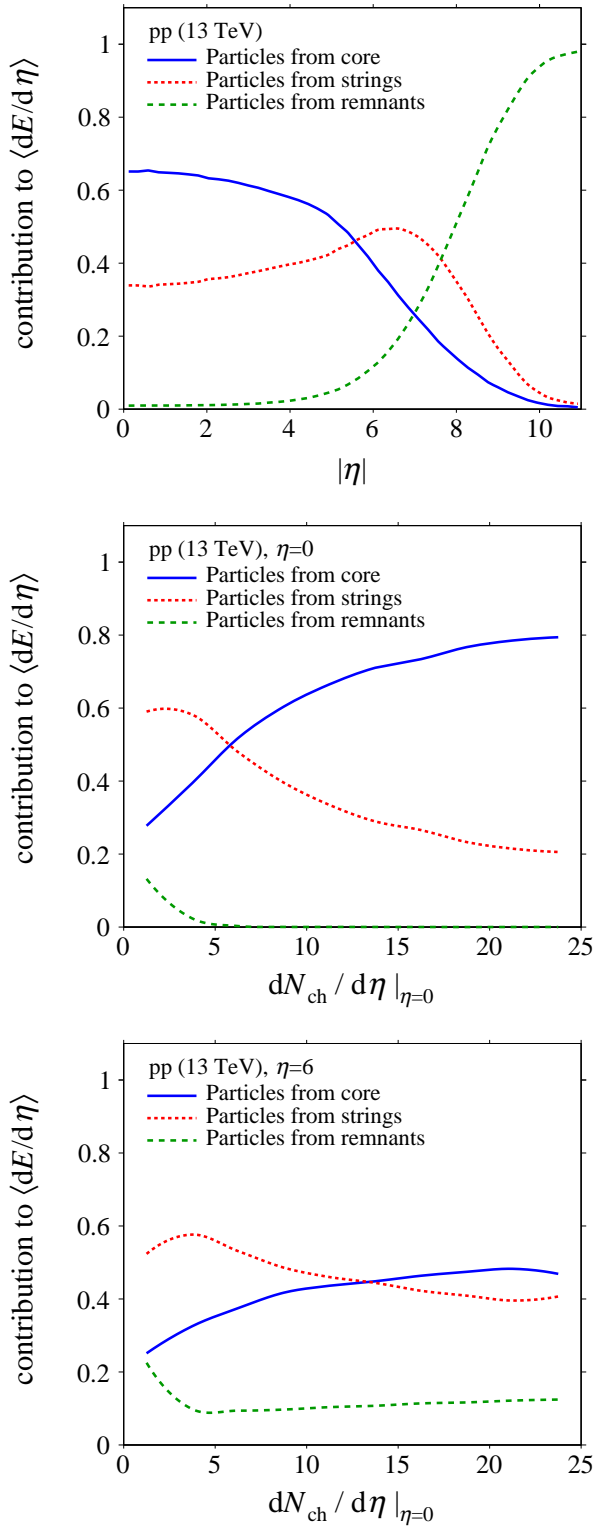


FIG. 5. Fractional contribution of particles originating from different production mechanisms to the total energy density $dE/d\eta$ as predicted by EPOS LHC. The top figure shows the contribution as function of $|\eta|$; the middle (bottom) figure shows the contributions at $\eta = 0$ ($\eta = 6$) as a function of the charged particle density at $\eta = 0$.

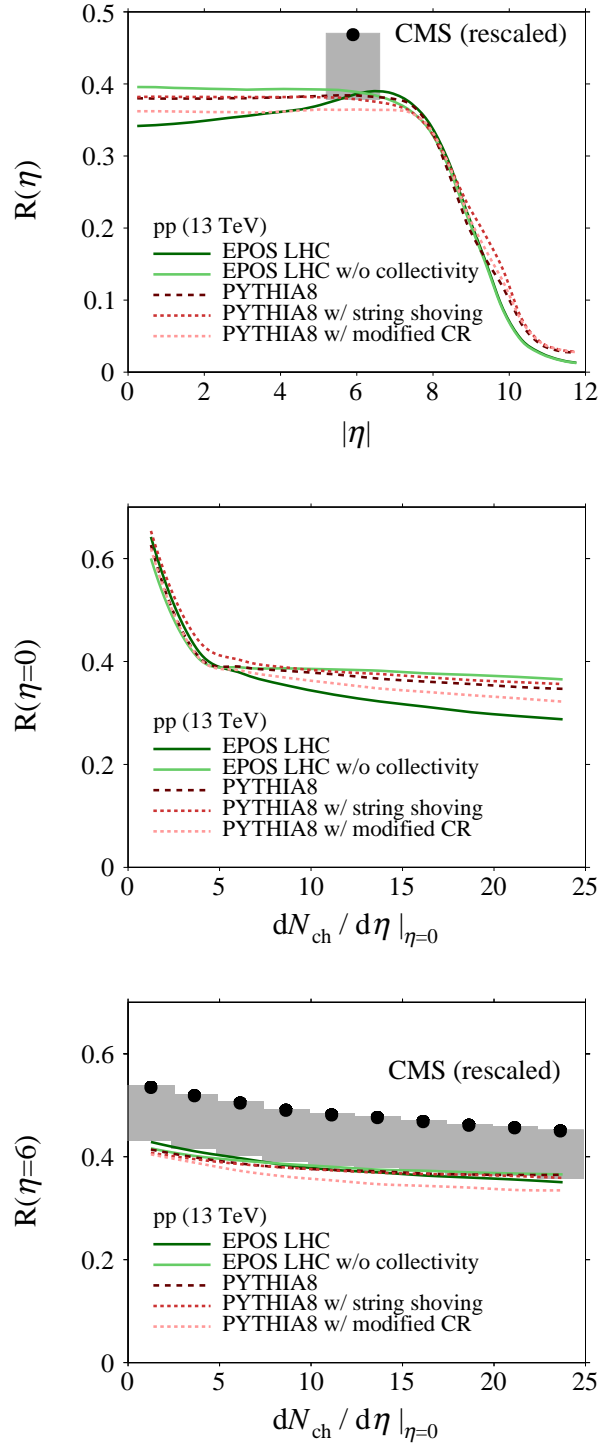


FIG. 6. Ratio of the average electromagnetic to hadronic energy densities R simulated for proton-proton collisions at 13 TeV with EPOS LHC (solid lines) with and without hydrodynamical treatment of the dense core, as well as PYTHIA8 (dashed lines) in the default configuration, with string shoving and with modified color reconnection (CR). The top figure shows $R(\eta)$ as function of $|\eta|$, the middle and bottom figure show R evaluated at $\eta = 0$ and $\eta = 6$ as a function of the central charged particle multiplicity. The asymmetric uncertainties of the CMS data are a feature of this measurement.

tuned and results should be treated with care but first observations, in particular about the characteristic shape of the distributions, can be made. It is interesting that we do not find a visible effect of the string shoving mechanism on the ratio of electromagnetic to hadronic energy, R , compared to the default string fragmentation (see Fig. 6). This is consistent with the predictions of EPOS LHC when statistical hadronization is disabled. These findings can be understood since in all these cases particle production is driven by QCD string fragmentation, which is well tuned to LEP data. Thus, what is found here is a characteristic feature of string fragmentation. If a microscopic collectivity model does not modify particle production by string fragmentation, as it is the case for string shoving, this has no impact on the observable R . With the modified color reconnection on the other hand, a reduced value of R is observed within $|\eta| < 7$ as well as a more prominent decrease of R at central rapidity as a function of $dN_{\text{ch}}/d\eta|_{\eta=0}$. This is due to enhanced baryon production as explained in Ref. [61]. Still, the decrease in R is not as strong as in EPOS LHC. More importantly, all configurations of PYTHIA8 exhibit a flat ratio as a function of pseudorapidity within $|\eta| < 7$. The value of R is a global feature of the hadronization and independent of rapidity. No transition from a statistical, to a string-dominated phase as in EPOS LHC is observed.

EPOS LHC was released after the first LHC data became available. At that time, only average values and the evolution of the mean transverse momentum as a function of the particle multiplicity were known precisely. The increase of multi-strange baryon production with particle multiplicity was a prediction of the model, but – as shown in Ref. [31] – was only qualitatively correct. Effectively, the core is formed in EPOS LHC only at larger multiplicities compared to what is necessary to reproduce the data. Thus, it is expected that the density needed to produce the core is currently overestimated and, as a consequence, the effect on muon production in air showers is significantly underestimated (not enough phase space for core hadronization). It would be useful to have precise data on R versus multiplicity to support (or reject) this hypothesis.

The study made with EPOS LHC and PYTHIA8 is just an example of what can be observed. A different model may have a different behavior, but it has been clearly demonstrated that R is sensitive to the type of hadronization. As a consequence, the observation of variations of the ratio of electromagnetic to hadronic energies as function of pseudorapidity or particle multiplicity is a strong test also of the nature of collective effects in proton-proton collisions (or other systems). Different implementations of statistical hadronization, QGP-like or macroscopic, can be distinguished. The proposed measurements will provide new constraints on the extension of the phase space in which statistical hadronization occurs, complementary to established measurements.

In any case, corresponding precision measurements of

R to 5% at the LHC seem feasible and could contribute significantly to a better understanding of muon production in air showers as described in section III in particular if the measurements could be done with a light-ion beam such as oxygen [67]. Despite the fact that calorimetric data are taken at various pseudorapidities (central and forward calorimeters), such ratios are not commonly published – with currently one notable exception [64]. The reverse argument also holds: in future huge-aperture air shower experiments, the tail of the $\ln N_{\mu}$ -distribution could be used to indirectly measure the slope of the energy distribution of neutral pions far beyond the reach of the LHC [10, 11].

V. SUMMARY

We have demonstrated that the muon production in air shower significantly depends on the ratio $R = E_{\text{em}}/E_{\text{had}}$, where E_{em} is the sum of energy in secondary γ (from π^0) and e^{\pm} while E_{had} is the sum of energy in hadrons in individual hadron collisions. We also showed that R itself depends on the hadronization mechanism. Thus, a change or transition in these mechanisms can help to explain the discrepancy between the observed number of muons in air showers by the Pierre Auger Observatory and the predictions based on current hadronic models. Since at the LHC, even in proton-proton interactions, one observes a transition from a string-type to a statistical-type hadronization at mid-rapidity, we used the particle ratios of the statistical model at all pseudorapidities to show that such hadronization scheme would in principle be sufficient to resolve the observed difference between simulations and cosmic ray data. Experimental measurements of R at the LHC are currently compatible with this possibility. On the other hand, extreme scenarios where full statistical hadronization is reached at low energies ($E_{\text{lab}} \sim \mathcal{O}(100 \text{ GeV})$) are already excluded by the slope of the energy-dependence of air shower muon data.

Furthermore, we discuss potential measurements of R at LHC, e.g. with calorimeters, as a function of pseudorapidity η or central charged particle multiplicity N_{ch} . We show that this observable can reveal properties of the nature of underlying fundamental particle production mechanisms. In particular we show that it provides a new handle to characterize mechanisms proposed for the explanation of statistical hadronization in proton-proton collisions. It is potentially possible to distinguish between quark-gluon-plasma-like (QGP-like) effects, as first known from heavy ion collisions, from alternative, more microscopic effects that do not require the formation of a QGP, see e.g. Refs. [32, 61].

Dedicated measurements at the LHC have now another opportunity to study collectivity in proton-proton collision using this observable. This will contribute to a better understanding of the mechanisms of hadronization in hadron collisions, and collectivity in proton-proton collisions or other light system. Measuring R at the LHC

potentially has a significant impact on resolving the current mystery of muon production in cosmic ray induced

extensive air showers. Thus, at last, one aspect to resolve the cosmic ray muon mystery is a better understanding of statistical hadronization in small collision systems.

-
- [1] A. Aab and others (Pierre Auger), The Pierre Auger Cosmic Ray Observatory, Nucl. Instrum. Meth. A **798**, 172 (2015).
- [2] J. Abraham and others (Pierre Auger), The Fluorescence Detector of the Pierre Auger Observatory, Nucl. Instrum. Meth. A **620**, 227 (2010).
- [3] H. Tokuno and others, New air fluorescence detectors employed in the Telescope Array experiment, Nucl. Instrum. Meth. A **676**, 54 (2012).
- [4] K.-H. Kampert and M. Unger, Measurements of the Cosmic Ray Composition with Air Shower Experiments, Astropart. Phys. **35**, 660 (2012).
- [5] A. Aab and others (Pierre Auger), Muons in air showers at the Pierre Auger Observatory: Mean number in highly inclined events, Phys. Rev. D **91**, 032003 (2015), [Erratum: Phys. Rev. D **91**, 059901 (2015)].
- [6] A. Aab and others (Pierre Auger), Testing Hadronic Interactions at Ultrahigh Energies with Air Showers Measured by the Pierre Auger Observatory, Phys. Rev. Lett. **117**, 192001 (2016).
- [7] R. U. Abbasi and others (Telescope Array), Study of muons from ultrahigh energy cosmic ray air showers measured with the Telescope Array experiment, Phys. Rev. D **98**, 022002 (2018).
- [8] H. P. Dembinski and others (EAS-MSU, IceCube, KASCADE-Grande, NEVOD-DECOR, Pierre Auger, SUGAR, Telescope Array, Yakutsk EAS Array), Report on Tests and Measurements of Hadronic Interaction Properties with Air Showers (2019) arXiv:1902.08124 [astro-ph.HE].
- [9] R. Ulrich, R. Engel, and M. Unger, Hadronic Multiparticle Production at Ultra-High Energies and Extensive Air Showers, Phys. Rev. D **83**, 054026 (2011).
- [10] L. Cazon, R. Conceio, and F. Riehn, Probing the energy spectrum of hadrons in proton air interactions at ultrahigh energies through the fluctuations of the muon content of extensive air showers, Phys. Lett. B **784**, 68 (2018).
- [11] L. Cazon, R. Conceio, M. A. Martins, and F. Riehn, Probing the π^0 spectrum at high- x in proton-Air interactions at ultra-high energies (2018) arXiv:1812.09121 [astro-ph.HE].
- [12] J. Adams and others (STAR), Experimental and theoretical challenges in the search for the quark gluon plasma: The STAR Collaboration's critical assessment of the evidence from RHIC collisions, Nucl. Phys. A **757**, 102 (2005).
- [13] K. Adcox and others (PHENIX), Formation of dense partonic matter in relativistic nucleus-nucleus collisions at RHIC: Experimental evaluation by the PHENIX collaboration, Nucl. Phys. A **757**, 184 (2005).
- [14] I. Arsene and others (BRAHMS), Quark gluon plasma and color glass condensate at RHIC? The Perspective from the BRAHMS experiment, Nucl. Phys. A **757**, 1 (2005).
- [15] B. B. Back and others, The PHOBOS perspective on discoveries at RHIC, Nucl. Phys. A **757**, 28 (2005).
- [16] K. Werner, I. Karpenko, and T. Pierog, The 'Ridge' in Proton-Proton Scattering at 7 TeV, Phys. Rev. Lett. **106**, 122004 (2011).
- [17] P. Bozek, Elliptic flow in proton-proton collisions at $\sqrt{s} = 7$ TeV, Eur. Phys. J. C **71**, 1530 (2011).
- [18] D. d'Enterria, G. K. Eyyubova, V. L. Korotkikh, I. P. Lokhtin, S. V. Petrushanko, L. I. Sarycheva, and A. M. Snigirev, Estimates of hadron azimuthal anisotropy from multiparton interactions in proton-proton collisions at $\sqrt{s} = 14$ TeV, Eur. Phys. J. C **66**, 173 (2010).
- [19] S. K. Prasad, V. Roy, S. Chattopadhyay, and A. K. Chaudhuri, Elliptic flow (v_2) in pp collisions at energies available at the CERN Large Hadron Collider: A hydrodynamical approach, Phys. Rev. C **82**, 024909 (2010).
- [20] G. Ortona, G. S. Denicol, P. Mota, and T. Kodama, Elliptic flow in high multiplicity proton-proton collisions at $\sqrt{s} = 14$ TeV as a signature of deconfinement and quantum energy density fluctuations, arXiv:0911.5158 [hep-ph] (2009).
- [21] L. Cunqueiro, J. Dias de Deus, and C. Pajares, Nuclear like effects in proton-proton collisions at high energy, Eur. Phys. J. C **65**, 423 (2010).
- [22] V. Khachatryan and others (CMS), Observation of Long-Range Near-Side Angular Correlations in Proton-Proton Collisions at the LHC, JHEP **09**, 091.
- [23] K. Dusling, W. Li, and B. Schenke, Novel collective phenomena in high-energy proton-proton and proton-nucleus collisions, Int. J. Mod. Phys. E **25**, 1630002 (2016).
- [24] C. Loizides, Experimental overview on small collision systems at the LHC, Nucl. Phys. A **956**, 200 (2016).
- [25] E. V. Shuryak, Quantum Chromodynamics and the Theory of Superdense Matter, Phys. Rept. **61**, 71 (1980).
- [26] H. Stöcker and W. Greiner, High-Energy Heavy Ion Collisions: Probing the Equation of State of Highly Excited Hadronic Matter, Phys. Rept. **137**, 277 (1986).
- [27] P. F. Kolb and U. W. Heinz, Hydrodynamic description of ultrarelativistic heavy ion collisions, in *Quark Gluon Plasma 3* (2003) pp. 634–714, arXiv:nucl-th/0305084 [nucl-th].
- [28] B. I. Abelev and others (STAR), Long range rapidity correlations and jet production in high energy nuclear collisions, Phys. Rev. C **80**, 064912 (2009).
- [29] G. Aad and others (ATLAS), Observation of a Centrality-Dependent Dijet Asymmetry in Lead-Lead Collisions at $\sqrt{s_{NN}} = 2.77$ TeV with the ATLAS Detector at the LHC, Phys. Rev. Lett. **105**, 252303 (2010).
- [30] S. Chatrchyan and others (CMS), Observation and studies of jet quenching in PbPb collisions at $\sqrt{s_{NN}} = 2.76$ TeV, Phys. Rev. C **84**, 024906 (2011).
- [31] J. Adam and others (ALICE), Enhanced production of multi-strange hadrons in high-multiplicity proton-proton collisions, Nature Phys. **13**, 535 (2017).
- [32] C. Bierlich, G. Gustafson, and L. Lönnblad, Collectivity without plasma in hadronic collisions, Phys. Lett. B **779**, 58 (2018).

- [33] B. Blok, C. D. Jkel, M. Strikman, and U. A. Wiedemann, Collectivity from interference, *J. High Energy Phys.* **2017** (12), 074.
- [34] T. Pierog, B. Guiot, I. Karpenko, G. Sophys, M. Stefaniak, and K. Werner, EPOS 3 and Air Showers, *EPJ Web Conf.* **210**, 02008 (2019).
- [35] L. A. Anchordoqui, C. Garcia Canal, S. J. Sciutto, and J. F. Soriano, Through the Looking-Glass with ALICE into the Quark-Gluon Plasma: A New Test for Hadronic Interaction Models Used in Air Shower Simulations, arXiv:1907.09816 [hep-ph] (2019).
- [36] T. Pierog and K. Werner, Muon Production in Extended Air Shower Simulations, *Phys. Rev. Lett.* **101**, 171101 (2008).
- [37] J. Matthews, A Heitler model of extensive air showers, *Astropart. Phys.* **22**, 387 (2005).
- [38] T. Pierog, I. Karpenko, J. M. Katzy, E. Yatsenko, and K. Werner, EPOS LHC: Test of collective hadronization with data measured at the CERN Large Hadron Collider, *Phys. Rev. C* **92**, 034906 (2015).
- [39] T. Bergmann, R. Engel, D. Heck, N. N. Kalmykov, S. Ostapchenko, T. Pierog, T. Thouw, and K. Werner, One-dimensional Hybrid Approach to Extensive Air Shower Simulation, *Astropart. Phys.* **26**, 420 (2007).
- [40] P. Abreu and others (Pierre Auger), Interpretation of the Depths of Maximum of Extensive Air Showers Measured by the Pierre Auger Observatory, *J. Cosmol. Astropart. Phys.* **2013** (02), 026.
- [41] H. P. Dembinski, Computing mean logarithmic mass from muon counts in air shower experiments, *Astropart. Phys.* **102**, 89 (2018).
- [42] A. Andronic, P. Braun-Munzinger, K. Redlich, and J. Stachel, Hadron yields, the chemical freeze-out and the QCD phase diagram, *J. Phys. Conf. Ser.* **779**, 012012 (2017).
- [43] K. Werner, A. G. Knospe, C. Markert, B. Guiot, I. Karpenko, T. Pierog, G. Sophys, M. Stefaniak, M. Bleicher, and J. Steinheimer, Resonance production in high energy collisions from small to big systems, *EPJ Web Conf.* **17**, 10900 (2018).
- [44] K. Werner, Core-Corona separation in ultra-relativistic heavy ion collisions, *Phys. Rev. Lett.* **98**, 152301 (2007).
- [45] J. Manninen and F. Becattini, Chemical freeze-out in ultra-relativistic heavy ion collisions at $s(\text{NN})^{1/2} = 130$ and 200-GeV, *Phys. Rev. C* **78**, 054901 (2008).
- [46] F. Becattini and J. Manninen, Strangeness production from SPS to LHC, *J. Phys. G* **35**, 104013 (2008).
- [47] J. Aichelin and K. Werner, Is the centrality dependence of the elliptic flow v_2 and of the average $\langle p_T \rangle$ more than a Core-Corona Effect?, *Phys. Rev. C* **82**, 034906 (2010).
- [48] J. Aichelin and K. Werner, Centrality Dependence of Strangeness Enhancement in Ultrarelativistic Heavy Ion Collisions: A Core-Corona Effect, *Phys. Rev. C* **79**, 064907 (2009), [Erratum: *Phys. Rev. C* **81**, 029902(E) (2010)].
- [49] S. Ostapchenko, On the re-summation of enhanced Pomeron diagrams, *Phys. Lett. B* **636**, 40 (2006).
- [50] S. Ostapchenko, Total and diffractive cross sections in enhanced Pomeron scheme, *Phys. Rev. D* **81**, 114028 (2010).
- [51] J. F. Soriano, L. A. Anchordoqui, T. C. Paul, and T. J. Weiler, Probing QCD approach to thermal equilibrium with ultrahigh energy cosmic rays, *PoS ICRC2017*, 342 (2018).
- [52] J. Alvarez-Muniz, L. Cazon, R. Conceição, J. D. de Deus, C. Pajares, and M. Pimenta, Muon production and string percolation effects in cosmic rays at the highest energies, arXiv:1209.6474 [hep-ph] (2012).
- [53] G. R. Farrar and J. D. Allen, A new physical phenomenon in ultra-high energy collisions, *EPJ Web Conf.* **53**, 07007 (2013).
- [54] L. A. Anchordoqui, H. Goldberg, and T. J. Weiler, Strange fireball as an explanation of the muon excess in Auger data, *Phys. Rev. D* **95**, 063005 (2017).
- [55] D. LaHurd and C. E. Covault, Exploring Potential Signatures of QGP in UHECR Ground Profiles, *J. Cosmol. Astropart. Phys.* **2018** (11), 007.
- [56] T. Sjöstrand, S. Mrenna, and P. Z. Skands, PYTHIA 6.4 Physics and Manual, *J. High Energy Phys.* **2006** (05), 026.
- [57] T. Sjöstrand, S. Ask, J. R. Christiansen, R. Corke, N. Desai, P. Ilten, S. Mrenna, S. Prestel, C. O. Rasmussen, and P. Z. Skands, An Introduction to PYTHIA 8.2, *Comput. Phys. Commun.* **191**, 159 (2015).
- [58] H. J. Drescher, M. Hladik, S. Ostapchenko, T. Pierog, and K. Werner, Parton based Gribov-Regge theory, *Phys. Rept.* **350**, 93 (2001).
- [59] B. Andersson, G. Gustafson, G. Ingelman, and T. Sjöstrand, Parton Fragmentation and String Dynamics, *Phys. Rept.* **97**, 31 (1983).
- [60] A. Ortiz Velasquez, P. Christiansen, E. Cuautle Flores, I. A. Maldonado Cervantes, and G. Paíć, Color Reconnection and Flowlike Patterns in pp Collisions, *Phys. Rev. Lett.* **111**, 042001 (2013).
- [61] C. Bierlich and J. R. Christiansen, Effects of color reconnection on hadron flavor observables, *Phys. Rev. D* **92**, 094010 (2015).
- [62] K. Werner, B. Guiot, I. Karpenko, and T. Pierog, Analysing radial flow features in p-Pb and p-p collisions at several TeV by studying identified particle production in EPOS3, *Phys. Rev. C* **89**, 064903 (2014).
- [63] C. Baus, R. Ulrich, and T. Pierog, The Cosmic Ray Monte Carlo package, <https://web.ikp.kit.edu/rulrich/crmc.html> (2014).
- [64] A. M. Sirunyan and others (CMS), Measurement of the average very forward energy as a function of the track multiplicity at central pseudorapidities in proton-proton collisions at $\sqrt{s} = 13$ TeV, *Eur. Phys. J. C* **79**, 893 (2019).
- [65] C. Bierlich and others, Robust Independent Validation of Experiment and Theory: Rivet version 3, *SciPost Phys.* **8**, 026 (2020).
- [66] From PYTHIA8 manual: Option `ColourReconnection:mode=1` aka “The new QCD based scheme”.
- [67] Z. Citron and others, Future physics opportunities for high-density QCD at the LHC with heavy-ion and proton beams, *CERN Yellow Rep. Monogr.* **7**, 1159 (2019).